Dynamical screening and quasiparticle spectral functions for nonmetals

F. Bechstedt, M. Fiedler, and C. Kress
Friedrich-Schiller-Universität, Max-Wien-Platz 1, 07743 Jena, Germany

R. Del Sole
Dipartimento di Fisica, II Universita degli Studi di Roma, Via della Ricerca Scientifica, I-00173 Roma, Italy
(Received 28 May 1993; revised manuscript received 19 October 1993)

Quasiparticle band-structure calculations for semiconductors treat the exchange-correlation self-energy operator within the *GW* approximation. In this paper, a detailed study of the energy dependence of the self-energy due to dynamical screening is presented. Spectral functions for near-band-gap excitations in silicon and diamond are calculated and the quasiparticle peak and satellite structures are discussed.

In order to describe the excitation energies of semiconducting or insulating solids in a reasonable manner the quasiparticle (QP) theory[1] has to be applied. The single-particle energy excitation spectrum is determined by the poles of the corresponding exact Green's function G. Apart from the Hartree contribution the electron-electron interaction is included in a self-energy Σ. For solids Hedin[2] proposed the linear expansion $\Sigma = GW$ of the exchange and correlation (XC) electron self-energy in terms of the screened Coulomb potential W. Cancellation effects in the most prominent vertex corrections emphasize the quality of the restriction to linear terms.[3] After first attempts, Hybertsen and Louie[4] have recently shown that the *GW* approximation is a reasonable approach to the true effect of XC on the single-particle energy within the framework of the first-principle pseudopotential method. They started from the results of the density-functional theory (DFT) in the local-density approximation (LDA) and treated the effects of XC beyond the DFT LDA in a perturbational-theory manner. Other authors[4–7] followed more or less this line with deviations in the treatment of the dynamical screening in the system.

Performing this procedure, in general, the full dynamics of the screening has to be taken into the screened potential W and hence into the full self-energy. The dynamical behavior of the self-energy itself gives rise to an energy dependence. It influences not only the position of the QP peak in the spectral function of the one-particle Green's function G. The strength of the QP peak is reduced, indicating the appearance of satellite structures. Typical values of this reduction are about 20%. Several questions arise from this fact. One is concerned with whether the approximated Green's function can be used in the self-energy calculation, or more strictly speaking, whether the reduced strength yields a reduction of the QP shift from the DFT LDA value via the Green's function in the *GW* representation. Furthermore, the relation of the QP peak and the accompanying satellites should be clarified. For this purpose, we analyze the dynamical behavior of XC self-energy Σ of electrons and holes in a nonmetal in more detail. Consequences for the approximation and the single-particle spectra are explicitly studied for the near-band-gap excitations in silicon and diamond.

Within a diagonal Bloch representation the Dyson equation for the QP Green's function can be written in the form[4]

$$G_{nn}(\mathbf{k},E) = G_{nn}^{\mathrm{DFT}}(\mathbf{k},E) + G_{nn}^{\mathrm{DFT}}(\mathbf{k},E)\delta\Sigma_{nn}(\mathbf{k},E) \times G_{nn}(\mathbf{k},E), \quad (1)$$

where the off-diagonal Bloch elements with respect to the band index n of the perturbation operator

$$\delta\Sigma(\mathbf{x},\mathbf{x}';E) = \Sigma(\mathbf{x},\mathbf{x}';E) - V_{\mathrm{XC}}(\mathbf{x})\delta(\mathbf{x}-\mathbf{x}') \quad (2)$$

are neglected. This assumption is in agreement with the findings of the near equivalence of QP and DFT LDA wave functions $\psi_{n\mathbf{k}}(\mathbf{x})$.[4] The perturbation is defined with respect to potential $V_{\mathrm{XC}}(\mathbf{x})$, which describes the XC effects within the DFT LDA.

Despite the band diagonalization the Dyson equation (1) can only be solved approximately via an iteration procedure since the perturbation itself is a functional of the Green's function. To accelerate the convergence of the iterative solution we apply a method developed by Blomberg and Bergersen[8,9] in the case of the homogeneous electron gas and later refined for core holes (cf. Ref. 10 and references therein). A Green's function

$$G_{nn}^{0}(\mathbf{k},E) = \frac{1}{E-\varepsilon_n(\mathbf{k})-i\eta_{n\mathbf{k}}} \quad (3)$$

is introduced with $\eta_{n\mathbf{k}} = +\delta$ $(\eta_{n\mathbf{k}} = -\delta), \delta \to +0$, for energies below (above) the chemical potential μ of the inhomogeneous electron gas.

The band energies $\varepsilon_n(\mathbf{k})$ are already shifted by a certain QP shift $\delta_n(\mathbf{k})$ with respect to the DFT LDA values $\varepsilon_n^{\mathrm{DFT}}(\mathbf{k})$. According to an idea of Hedin,[1,2] this shift has to be calculated self-consistently. Later it has been taken up also by other authors[11,12] in the case of the homogeneous electron gas or simple metals. The Dyson equation (1) changes into

$$G_{nn}(\mathbf{k},E) = G^0_{nn}(\mathbf{k},E) + G^0_{nn}(\mathbf{k},E)\{\delta\Sigma_{nn}(\mathbf{k},E) - \delta_n(\mathbf{k})\} \times G_{nn}(\mathbf{k},E). \quad (4)$$

This equation represents a suitable starting point for an iterative solution. Restricting to the first nonvanishing order with respect to $\{\delta\Sigma_{nn}(\mathbf{k},E) - \delta_n(\mathbf{k})\}$ one obtains

$$G_{nn}(\mathbf{k},E) = G^0_{nn}(\mathbf{k},E) + \left\{\delta\Sigma^0_{nn}(\mathbf{k},E) - \delta_n(\mathbf{k})\right\}\left[G^0_{nn}(\mathbf{k},E)\right]^2, \quad (5)$$

where the Green's function in the self-energy has to be replaced by G^0. To avoid the unphysical double pole at $E = \varepsilon_n(\mathbf{k})$ in the second term on the right-hand side one has to take

$$\delta_n(\mathbf{k}) = \mathrm{Re}\delta\Sigma^0_{nn}(\mathbf{k},\varepsilon_n(\mathbf{k})). \quad (6)$$

To simplify the considerations we have assumed that the quasiparticle described by the Green's function (3) is undamped, i.e., $\mathrm{Im}\Sigma^0_{nn}(\mathbf{k},\varepsilon_n(\mathbf{k})) \equiv 0$. In the explicit calculations, where we apply a screening function in the plasmon-pole approximation, this assumption is practically always fulfilled.

Together with expression (2) this equation gives a clear definition of a QP shift of a band state. However, the matrix element of the self-energy change depends on $\delta_n(\mathbf{k})$ itself via the Green's function G^0. Consequently, the QP shifts $\delta_n(\mathbf{k})$ and the QP band energies $\varepsilon_n(\mathbf{k})$, respectively, have to be determined self-consistently. On the other hand, the appearance of G^0 [Eq. (3)] in the QP-shift definition [Eq. (5)] indicates that there is no reduction of the QP shift by dynamical screening effects so far the function G^0 is really taken at the QP energy $\varepsilon_n(\mathbf{k})$ itself and not at other energies, e.g., $\varepsilon^{\mathrm{DFT}}_n(\mathbf{k})$.

Contrary to the QP shift (6) the spectral function $A_n(\mathbf{k},E)$ of the diagonal Green's function $G_{nn}(\mathbf{k},E)$,

$$G_{nn}(\mathbf{k},E) = \int_{-\infty}^{+\infty} dE' \frac{A_n(\mathbf{k},E')}{E - E' + i\delta\mathrm{sgn}(E'-\mu)} \quad (\delta \to +0), \quad (7)$$

is much more influenced by the energy dependence of the self-energy resulting from the dynamics in the screening. After the first iteration we derive from Eq. (5)

$$A_n(\mathbf{k},E) = \left[1 + \frac{\partial}{\partial E}\mathrm{Re}\Sigma^0_{nn}(\mathbf{k},E)\right]\delta(E - \varepsilon_n(\mathbf{k})) + \mathrm{sgn}(E-\mu)\left[\frac{\partial}{\partial E}\frac{P}{E-\varepsilon_n(\mathbf{k})}\right] \times \frac{1}{\pi}\mathrm{Im}\Sigma^0_{nn}(\mathbf{k},E). \quad (8)$$

The spectral function represents a sharp peak at the QP energy $\varepsilon_n(\mathbf{k})$ with a reduced spectral weight and additional broad peaks at shifted energies. The additional peaks describe satellite structures related to shakeup excitations.[1,13] For the purpose of the preparation of a more complete spectral representation (7) it is convenient and physically appealing to divide each matrix element of the self-energy into the energy-independent bare exchange (X) term and the energy-dependent correlation (C) part which contains the dynamical effects of screening:

$$\Sigma^0_{nn}(\mathbf{k},E) = \Sigma^X_n(\mathbf{k}) + \Sigma^C_n(\mathbf{k},E). \quad (9)$$

The correlation part of the self-energy fulfills a similar spectral representation as the QP Green's function in Eq. (7). The corresponding spectral function $\Gamma_n(\mathbf{k},E)$ can be written as

$$\Gamma_n(\mathbf{k},E) = -\frac{1}{V}\sum_{\mathbf{q}}\sum_{\mathbf{G},\mathbf{G}'}\frac{4\pi e^2}{|\mathbf{q}+\mathbf{G}||\mathbf{q}+\mathbf{G}'|}\sum_{n',\mathbf{k}'}B^{\mathbf{k}\mathbf{k}'}_{nn'}(\mathbf{q}+\mathbf{G})B^{\mathbf{k}\mathbf{k}'*}_{nn'}(\mathbf{q}+\mathbf{G}')\frac{1}{\pi}\mathrm{Im}\epsilon^{-1}(\mathbf{q}+\mathbf{G},\mathbf{q}+\mathbf{G}';E-\varepsilon_{n'}(\mathbf{k}')) \times\left[\Theta(E-\varepsilon_{n'}(\mathbf{k}'))\Theta(\varepsilon_{n'}(\mathbf{k}')-\mu) - \Theta(\varepsilon_{n'}(\mathbf{k}')-E)\Theta(\mu-\varepsilon_{n'}(\mathbf{k}'))\right], \quad (10)$$

where the Bloch matrix elements $B^{\mathbf{k}\mathbf{k}'}_{nn'}(\mathbf{q}+\mathbf{G})$ of plane waves are introduced. The wave vector $\mathbf{q}$ runs throughout the Brillouin zone whereas the vectors $\mathbf{G},\mathbf{G}'$ are elements of the reciprocal Bravais lattice. V denotes the crystal volume. The behavior of the spectral function is governed by the wave-vector- and frequency-dependent inverse dielectric function ϵ^{-1}.

By means of the spectral function (10) of the correlation self-energy the spectral function (8) of a quasiparticle in a Bloch state $n\mathbf{k}$ can be transformed into a more familiar form

$$A_n(\mathbf{k},E) = \left[1 - \int_{-\infty}^{+\infty} dE' \frac{\Gamma_n(\mathbf{k},E'+\varepsilon_n(\mathbf{k}))}{E'^2}\right]\delta(E-\varepsilon_n(\mathbf{k})) + \int_{-\infty}^{+\infty} dE' \frac{\Gamma_n(\mathbf{k},E'+\varepsilon(\mathbf{k}))}{E'^2}\delta(E-\varepsilon_n(\mathbf{k})-E'). \quad (11)$$

The expression (11) of the QP spectral function represents a linear expansion of a more general result[10,13]

$$A_n(\mathbf{k},E) = \int_{-\infty}^{+\infty}\frac{dt}{2\pi\hbar}e^{\frac{i}{\hbar}[E-\varepsilon_n(\mathbf{k})]t}e^{-C_n(\mathbf{k},t)}, \quad (12)$$

$$C_n(\mathbf{k},t) = \int_{-\infty}^{+\infty} dE' \frac{\Gamma_n(\mathbf{k},E'+\varepsilon_n(\mathbf{k}))}{E'^2}\left[1 - e^{-\frac{i}{\hbar}E't}\right], \quad (13)$$

with respect to the so-called satellite generator

$C_n(\mathbf{k},t)$,[14] which is an integral over linked diagrams of the screened interaction.

A rigorous proof of representation (12) for arbitrary band states and screening models cannot be given by the continuation of the iteration procedure according to Eq. (5). This is only possible in an approximate manner. An exact proof has been given for dispersionless bands, e.g., core levels, with strongly localized wave functions and δ-function-like behavior of the imaginary part of the screening function (see Refs. 10, 13, and 14 and references therein). For band states the main difficulties arise from the momentum changes of the particles. Approximate treatments for band states follow the exactly solvable case as closely as possible, but partially neglect the recoil effect in the energy denominators to obtain a solution in a closed form. One example is the calculation of the electron Green's function for metals by Hedin.[15] An elegant way to derive expression (12) has been demonstrated by Almbladh and Hedin.[16] They started from an equation of motion for the logarithm of the Green's function, the main time dependence of which is already separated. In the term generating the satellites the full Green's functions are approximated by the start function of Eq. (3).

The satellite generator in Eq. (13), which is only related to the spectral function of the correlation self-energy, involves the deviation of the line shape from a single δ function. That particularly concerns the reduction of the spectral strength of the main peak at the position of the QP energy, $E=\varepsilon_n(\mathbf{k})$, and the corresponding redistribution of states into the satellite structures. Consequently the generalized spectral function (12) of a quasiparticle also fulfills important sum rules, in contrast to the iterative solution (11). It holds

$$1=\int_{-\infty}^{+\infty} dE A_n(\mathbf{k},E), \tag{14}$$

$$\varepsilon_n^{\mathrm{HF}}(\mathbf{k})=\int_{-\infty}^{+\infty} dE E A_n(\mathbf{k},E), \tag{15}$$

where the band energy in the Hartree-Fock approximation $\varepsilon_n^{\mathrm{HF}}(\mathbf{k})=\varepsilon_n(\mathbf{k})-i\hbar\frac{\partial}{\partial t}C_n(\mathbf{k},t)|_{t=0}=\varepsilon_n(\mathbf{k})-\mathrm{Re}\Sigma_n^C(\mathbf{k},\varepsilon_n(\mathbf{k}))$ is introduced. The sum rule (15) gives insight into Koopman's theorem, even when correlation is taken into account. The energy of an excited electron (hole) is not $\varepsilon_n^{\mathrm{HF}}(\mathbf{k})$ but, rather electrons (holes) appear with energies $\varepsilon_n(\mathbf{k})$ or at shifted positions in the satellite structures. However, the center of gravity of all excitations is again governed by $\varepsilon_n^{\mathrm{HF}}(\mathbf{k})$.

The reduction of the spectral strength of the main QP peak can be described by the so-called QP renormalization factor $z_n(\mathbf{k})$.[1,4] In contrast to the first iteration in Eq. (8) the spectral function (12) gives rise to a strength of the QP peak at $E=\varepsilon_n(\mathbf{k})$ of

$$z_n(\mathbf{k})=\exp\left[-\beta_n(\mathbf{k})\right], \tag{16}$$

$$\beta_n(\mathbf{k})=-\frac{\partial}{\partial E}\mathrm{Re}\Sigma_n^C(\mathbf{k},E) \qquad [E=\varepsilon_n(\mathbf{k})]. \tag{17}$$

That can be shown by expansion of $e^{-C_n(\mathbf{k},t)}$ in Eq. (12) in a power series and by consideration of the time-independent contribution. According to the iteration procedure in Eq. (4), in which the starting Green's function already contains QP effects, the definition in Eq. (16) is somewhat different from that usually obtained,[1,4] considering only a spectral function with one pole and a self-energy $\sim G^{\mathrm{DFT}}W$. In this case one has $z_n(\mathbf{k})=\left[1-\frac{\partial}{\partial E}\mathrm{Re}\Sigma_n^C(\mathbf{k},E)\right]^{-1}$ $[E=\varepsilon_n(\mathbf{k})]$. Since, however, in general $-\frac{\partial}{\partial E}\mathrm{Re}\Sigma_n^C(\mathbf{k},E)\ll 1$ $[E=\varepsilon_n(\mathbf{k})]$ holds, the different strength definitions do not give rise to very different results and agree within the linear approximation.

In order to discuss the XC self-energy and the resulting QP self-energy we focus our attention on the highest occupied state Γ'_{25v} and the lowest unoccupied state X_{1c} of silicon and diamond. The small displacement of the last state on the Δ line from X towards Γ is disregarded. We perform a model calculation for the self-energy. The electronic structure is calculated by means of a tight-binding method using a minimum Gaussian basis set but taking the full overlap into account.[17] The screened potential is described within a generalized plasmon-pole model. The diagonal dielectric function well describes the screening in the whole wave-vector region.[18] Off-diagonal elements are included taking the plasmon-pole frequency $\Omega(\mathbf{q}+\frac{1}{2}(\mathbf{G}+\mathbf{G}'))$ at the averaged wave vector. To model the distribution of the energy losses over different frequencies a certain broadening Γ of the plasmon peak is considered.

For the discussion of the analytical properties of electron and hole self-energies we have plotted the real and imaginary parts of the correlation self-energy of the X_{1c} state and the Γ'_{25v} state as examples for electrons and holes in Figs. 1 and 2. More precisely, the modulus of the imaginary part is shown since apart from a factor π it represents the spectral function from Eq. (10). For numerical reasons we consider a finite lifetime parameter δ for both particles. The second curve in each figure represents screening which is characterized by a broadened plasmon peak.

In the imaginary parts in Figs. 1(b) and 2(b) we find two peaks located nearly at the energies $E=\varepsilon_n(\mathbf{k})\pm\hbar\Omega_{\mathrm{eff}}$, where Ω_{eff} represents an effective plasmon frequency somewhat larger than $\Omega(0)$. These peaks are broadened. In the case of δ-like plasmon poles in the screening function the broadening is mainly due to additional peaks at $E=\varepsilon_n(\mathbf{k})-[\varepsilon_n(\mathbf{k})-\varepsilon_{n'}(\mathbf{k}')]\pm\hbar\Omega_{\mathrm{eff}}$. They indicate further decay channels for electrons $[\varepsilon_n(\mathbf{k})>\mu]$ and holes $[\varepsilon_n(\mathbf{k})<\mu]$ in which electron-hole pairs with energies $\varepsilon_n(\mathbf{k})-\varepsilon_{n'}(\mathbf{k}')$ are annihilated or created besides the plasmons. The strength of the additional peaks is smaller because of the fact that it holds $|B_{nn'}^{\mathbf{kk}'}(\mathbf{q})|\ll|B_{nn}^{\mathbf{kk}'}(\mathbf{q})|$ for not too large $|\mathbf{q}|$ and $n\neq n'$. The strength of two structures around the QP energy $\varepsilon_n(\mathbf{k})$ is different. Between the two resonances around $E=\mu$ and $E=\varepsilon_n(\mathbf{k})$ the imaginary parts vanish or are at least rather small. This behavior observed generally for $\mathrm{Im}\Sigma_n^C(\mathbf{k},E)$ is similar to that calculated for the interacting electron gas[1] for which $\mathrm{Im}\Sigma_n^C(\mathbf{k},\mu)=0$. However, the details of the energy dependence in this region vary somewhat with the specification of the screening

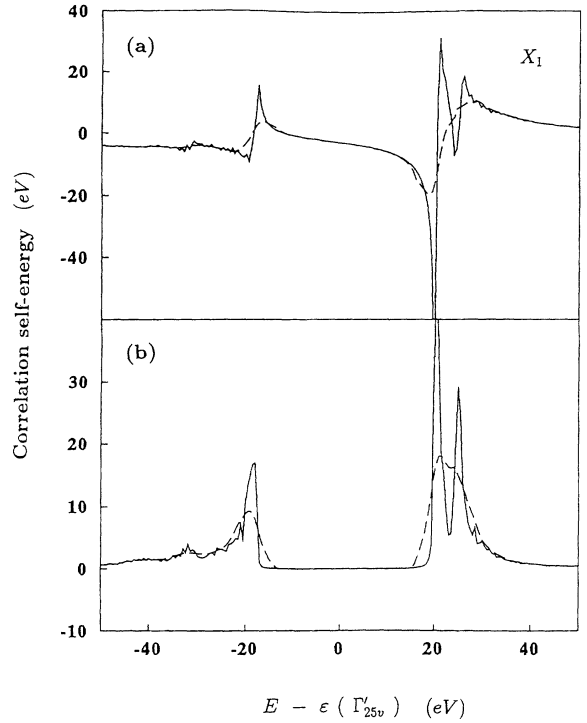

FIG. 1. (a) Real part $\mathrm{Re}\Sigma_n^C(\mathbf{k},E)$ and (b) imaginary part $|\mathrm{Im}\Sigma_n^C(\mathbf{k},E)|$ of the correlation self-energy for X_{1c} electron states in silicon. Different particle and plasmon-pole broadenings are considered. Solid line, $\delta = 0.1$ eV and $\Gamma = 0$; dashed line, $\delta = 0.1$ eV and $\Gamma = 2$ eV.

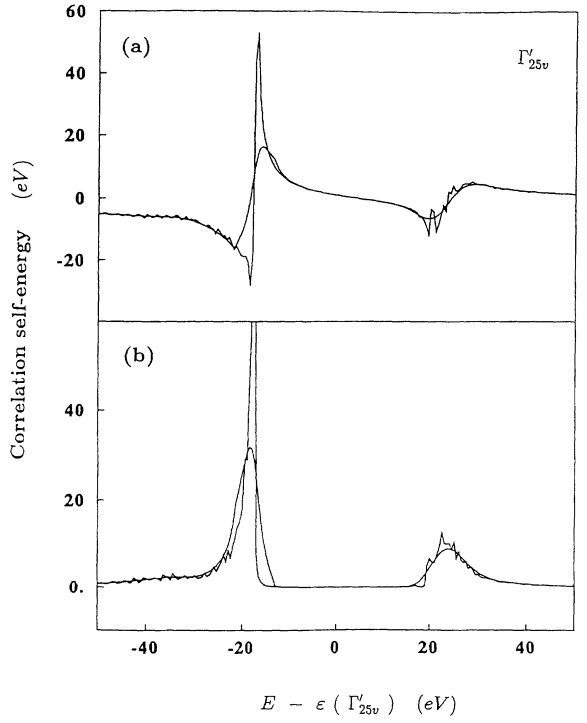

FIG. 2. (a) Real part $\mathrm{Re}\Sigma_n^C(\mathbf{k},E)$ and (b) imaginary part $|\mathrm{Im}\Sigma_n^C(\mathbf{k},E)|$ of the correlation self-energy for Γ'_{25v} hole states in silicon. Different particle and plasmon-pole broadenings are considered. Solid line, $\delta = 0.1$ eV and $\Gamma = 0$; dashed line, $\delta = 0.1$ eV and $\Gamma = 2$ eV.

and the band structure. For instance, we expect small structures for energies between the two resonances apart from an interval around μ given by the gap energy. They should arise from the electron-hole pair excitations in the screening function which, however, are neglected in the plasmon-pole approximation. We get an idea of this effect considering the curve for $\Gamma = 2$ eV, although there electron-hole pair energies with arbitrary energies appear due to the Lorentzian tail of the imaginary part in the screening function.

From the spectral representation, where the real part, $\mathrm{Re}\Sigma_n^C(\mathbf{k},E)$ is represented as a Hilbert transform of $|\mathrm{Im}\Sigma_n^C(\mathbf{k},E)|$, more precisely of the spectral function $\Gamma_n(\mathbf{k},E)$, an energy dependence of the real part of the self-energies follows as shown in Figs. 1(a) and 2(a). As in the imaginary parts we find structures of the oscillator form near $E = \varepsilon_n(\mathbf{k}) \pm \hbar\Omega_{\mathrm{eff}}$. The ratio of these structures is the same as already discussed for electrons and holes. Between the two structures, particularly for energies near the quasiparticle energy, the curves $\mathrm{Re}\Sigma_n^C(\mathbf{k},E)$ have a negative slope. Consequently the QP renormalization factors in Eq. (16) are smaller than unity. The energy dependences differ with respect to the higher derivatives. The curves $\mathrm{Re}\Sigma_n^C(\mathbf{k},E)$ are concave downwards for electron states and concave upwards for hole states.

Curves similar to those shown in Figs. 1 and 2 have been obtained for diamond. Only the abscissa is somewhat scaled because of the larger plasmon frequency. On the other hand, the variation of the correlation self-energy itself is weak since the polarization charges are not so very different. This fact can also be seen from the self-energies at the QP energies. For the two materials under consideration we find $\mathrm{Re}\Sigma_n^C(k,\varepsilon_n(\mathbf{k})) = -4.09$ (-4.89) eV (X_{1c}) and 0.27 (0.97) eV (Γ'_{25v}). Adding the negative exchange contributions $\Sigma_n^X(\mathbf{k}) = -15.35$ (-9.72) eV (X_{1c}) and -12.31 (-18.88) eV (Γ'_{25v}) to $\mathrm{Re}\Sigma_n^C(\mathbf{k},E)$, the crossing points with the straight lines $E - \varepsilon_n(\mathbf{k})$ give total self-energies of -10.44 (-14.61) eV (X_{1c}) and -12.04 (-17.91) (Γ'_{25v}) for silicon (diamond). These values approach the findings of Hybertsen and Louie,[4] especially in the Γ'_{25v}-hole case.

Consequences of the energy dependence of the correlation self-energy for the spectral behavior of electron and hole QP excitations are represented in Fig. 3. We have used the general expression (12) for the spectral function. The energy interval is restricted to the QP peak and the first satellite structures around the main peak.

In Fig. 3 the central peak of the spectral function $E = \varepsilon_n(\mathbf{k})$ show a Lorentzian shape according to the assumed small numerical broadening of $\delta = 0.1$ eV for the QP excitations. As a consequence of the behavior of the imaginary part of the dynamical correlation self-energy the satellite structures are centered around the energies $E = \varepsilon_n(\mathbf{k}) \pm \hbar\Omega_{\mathrm{eff}}$, or more precisely $E = \varepsilon_n(\mathbf{k}) + [\varepsilon_n(\mathbf{k}) - \varepsilon_{n'}(\mathbf{k}')] \pm \hbar\Omega_{\mathrm{eff}}$. This means that, whereas the main peak is formed by usual quasiparticles, i.e., bare (Hartree-Fock) particles dressed by a cloud of virtual plasmons and electron-hole pairs (if the single plasmon-pole approximation is overcome), the additional satellite structures may be interpreted by particles coupled to a cloud of real plasmons (and electron-hole pairs). We

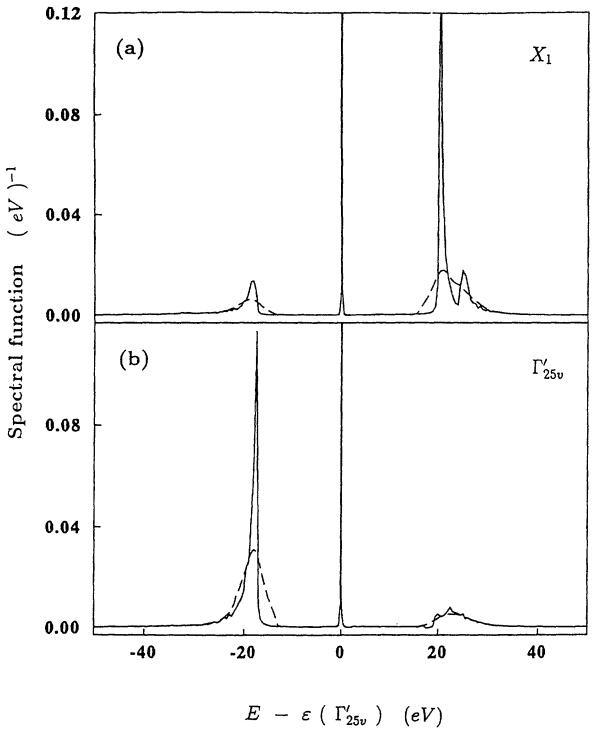

FIG. 3. (a) Electron and (b) hole spectral functions of silicon. The bottom of the conduction band X_{1c} and the top of the valence band Γ'_{25v} are considered. Solid line, $\delta = 0.1$ eV and $\Gamma = 0$, dashed line, $\delta = 0.1$ eV and $\Gamma = 2$ eV.

mention that the characteristic energy shift from the QP position is really given by $\hbar\Omega_{\text{eff}}$. This is due to the iteration procedure for the Green's function starting with expression (3). The introduction of the QP energy $\varepsilon_n(\mathbf{k})$ into the Green's function appearing in the self-energy avoids the plasmaron problem,[8,9] which means that the satellites occur closer to the main peak.

According to the discussion of the imaginary part of the dynamical correlation self-energy the strengths of the first-neighbor satellites (only considered here) are different. For electron (hole) states with $\varepsilon_n(\mathbf{k}) > \mu$ [$\varepsilon_n(\mathbf{k}) < \mu$] the satellite structure near $\varepsilon_n(\mathbf{k}) + \hbar\Omega_{\text{eff}}$ [$\varepsilon_n(\mathbf{k}) - \hbar\Omega_{\text{eff}}$] is stronger than that around $\varepsilon_n(\mathbf{k}) - \hbar\Omega_{\text{eff}}$ [$\varepsilon_n(\mathbf{k}) + \hbar\Omega_{\text{eff}}$]. The appearance of such a high-(low) energy peak is related to the dispersion of the bands. For dispersionless, strongly localized states with $\varepsilon_n(\mathbf{k}) = \varepsilon_n$ and $B^{\mathbf{kk}'}_{nn'}(\mathbf{q}+\mathbf{G}) \sim \delta_{nn'}$, these satellites even vanish. A satellite can be only observed at $E = \varepsilon_n + \text{sgn}(\varepsilon_n - \mu)\hbar\Omega_{\text{eff}}$ if, moreover, the dispersion of the plasmons is neglected. We remember that within such an approximation the spectral function in Eq. (12) can be described by Poisson-distributed δ functions at $E = \varepsilon_n + \text{sgn}(\varepsilon_n - \mu)N \cdot \hbar\Omega_{\text{eff}}$ ($N = 0,1,2,...$).[10,13] We point out that the strength of the satellite structures is remarkable. For the first structure considered here we find a ratio to the main QP peak of about $-\ln z_n(\mathbf{k})$ with $z_n(\mathbf{k})$ as the QP strength defined in Eq. (16). With characteristic values of the QP renormalization factors of $z_n(\mathbf{k}) = 0.80$ (0.86) for X_{1c} and $z_n(\mathbf{k}) = 0.78$ (0.86) for Γ'_{25v} of silicon (diamond) one derives ratios of about 0.25 (0.16) or 0.28 (0.16). These numbers indicate that dynamical effects in the wide-gap material diamond are somewhat reduced in comparison with silicon. Hence the satellite structures also play a more important role in the semiconductors with smaller plasmon frequency.

In conclusion, we have generalized an iteration procedure for the band–diagonal one-particle Green's function. Starting from a zero-order Green's function, which already contains the QP energy, we derive two important results. First, a spectral representation of the full Green's function follows that fulfills the important sum rules. The shape of the corresponding spectral function is only determined by the dynamical correlation, or more precisely the energy dependence of the pure correlation self-energy. On the other hand, the QP energy, i.e., the position of the main peak of the spectral function, is defined by both quantum-mechanical effects of the electron-electron interaction, (static) exchange, and (dynamical) correlation. Second, the QP shift of electrons and holes with respect to the DFT LDA values is related to the corresponding self-energy difference. Thereby, in the self-consistent calculation the Green's function in the *GW* expression can be replaced by the zero-order one. As a consequence of the applied iteration procedure, where the pole in the zero-order function is fixed at the QP energy itself and not at the corresponding DFT LDA energy, the QP shift is not reduced by the QP renormalization factor.

An important consequence of the dynamical screening is the energy dependence of the dynamical electron correlation. It determines the spectral behavior of the full Green's function via the pure correlation self-energy. The strengths of the main QP peak is reduced. The reduction is governed by the energy derivative of the real part of the correlation self-energy. Because of the conservation of the total strength satellite structures appear at other energies. They are directly related to the imaginary part of the correlation self-energy. The spectral behavior of the full Green's function around the QP energy differs very little from that obtained from the zero-order function. The main effect concerns the pole strength. On the other hand, in spectral regions at a distance of about the plasmon-pole energy, strong satellite structures appear and compensate for the loss of strength of the QP peak.

[1] L. Hedin and S. Lundqvist, Solid State Phys. **23**, 1 (1969).
[2] L. Hedin, Phys. Rev. **139**, A796 (1965).
[3] R. Daling, P. Unger, P. Fulde, and W. van Haeringen, Phys. Rev. B **43**, 1851 (1991).
[4] M.S. Hybertsen and S.G. Louie, Phys. Rev. Lett. **55**, 1418 (1985); Phys. Rev. B **34**, 5390 (1986).
[5] R.W. Godby, M. Schlüter, and L.J. Sham, Phys. Rev. B **35**, 4180 (1987); **37**, 10 159 (1988).
[6] W. von der Linden and P. Horsch, Phys. Rev. B **37**, 8351 (1988).
[7] R. Hott, Phys. Rev. B **44**, 1057 (1991).
[8] C. Blomberg and B. Bergersen, Can. J. Phys. **50**, 2286

(1972).
[9] B. Bergersen, F.W. Kus, and C. Blomberg, Can. J. Phys. **51**, 102 (1973).
[10] F. Bechstedt, Phys. Status Solidi B **112**, 9 (1982).
[11] P. Minnhagen, J. Phys. C **8**, 1535 (1975).
[12] D.R. Penn, Phys. Rev. Lett. **40**, 568 (1978).
[13] D.C. Langreth, Phys. Rev. B **1**, 471 (1970); in *Collective Properties of Physical Systems*, Nobel Symposia 24, edited by B.I. Lundqvist and S. Lundqvist (Academic Press, New York, 1973), p. 210.
[14] D.C. Langreth, in *Interaction of Radiation with Condensed Matter* (IAEA, Vienna, 1977), Vol. 1, p. 295.
[15] L. Hedin, Phys. Scr. **21**, 477 (1980).
[16] C.-O. Almbladh and L. Hedin, in *Handbook of Synchrotron Radiation*, edited by E.E. Koch (North-Holland, Amsterdam, 1983), Vol. 1, p. 607.
[17] C. Kress, M. Fiedler, and F. Bechstedt, Physica B **185**, 400 (1993).
[18] F. Bechstedt and R. Del Sole, Phys. Rev. B **38**, 7710 (1988).